

## Automatic Voltage Regulator Design Enhancement Taking Into Account Different Operating Conditions and Environment Disturbances

F. Ahcene<sup>(1)</sup>, H. Bentarzi<sup>(1)\*</sup>, A. Ouadi<sup>(1)</sup>

<sup>(1)</sup> Laboratory Signals and Systems, IGEE,  
University M'hamed Bougara, Boumerdes, Algeria

\*Corresponding author: h.bentarzi@univ-boumerdes.dz

### ARTICLE INFO

#### Article History :

Received : 03/01/2021

Accepted : 25/06/2021

#### Key Words:

Automatic Voltage Regulator AVR; synchronous generator; Particle Swarm Optimization PSO; excitation system; modeling and linearization; Active Disturbance Rejection Control ADRC; environment impact.

### ABSTRACT/RESUME

*Abstract: In large power systems as well as in micro-grids, the generation of electrical energy is ensured by the synchronous generators, the enhancement of their dynamic performance during disturbances is increasingly required. This research work aims to maintain the terminal voltage constant starting by a 1.5 k VA synchronous laboratory power machine with salient pole under different operating conditions and environment disturbances. Then, a second generator of 187 MVA with different exciting systems is studied. A voltage regulation is ensured by a well-known controller named Automatic Voltage Regulator (AVR). In the first method, this AVR is based on a conventional Proportional Integral (PI) controller. The used optimization method for the controller parameters determination is the Particle Swarm Optimization (PSO) algorithm. In the second method, the AVR is based on Active Disturbance Rejection Control (ADRC) that allows controlling uncertain systems, where the dynamic is not well defined as in this application. Both methods are tested under different operating conditions. The obtained simulation results are encouraged to validate the use of the ADRC control in such application.*

### I. Introduction

Since the electrical energy is a scarce and precious resource, investigation can be conducted into its use in the most optimal way possible.

For about two decades, the consumption of electricity has globally increased by a factor of 70. This increase is due to the increase in the standard of living and life expectancy of the people in the earth. However, these tremendous raises have been made with an increasingly significant impact on the environment, whether in the production, transport or in the use of this energy.

While waiting for renewable energies to take a place considerably, we must think about minimizing this effect; for example, more attention should be paid to reduce consumption, improving the efficiency of power plants, transmission and distribution networks, and also adopting specific compensation programs for CO<sub>2</sub> gases.

During the past decade, power utilities in Algeria have operated their power systems at full power and often closer to their stability limits. This phenomenon can damage the generator and the power grid components which in turn may affect on the environment.

Consequently, the regulation of the voltage at the terminals of the generator, despite the presence of disturbances has become a priority and a great concern. In practice, this role is devoted to the generator excitation system [1].

The efficiency of the power supply system and the stability of the synchronous generator are highly dependent on the reliability of the exciter which is the main part for generating the electrical energy from the whole generation system. Due to the fact that the excitation supports the stator and the rotor, however, the loss of excitation of the generator weakens the various parts of the machine and therefore leads to an imbalance of mechanical and

electrical power and the speed of the rotor increases above the synchronous speed [2]. The excitation system reduces these above mentioned risks, especially in the self-excited generator type. The significant advantage of this type can generate negative excitation current. Thus, it allows a rapid de-excitation which may be necessary during an internal fault of the generator and also reduces the response time in the controller and the size of the installation [13].

Therefore, an Automatic Voltage Regulator (AVR) is essential to achieve satisfactory system performance. This AVR is generally based on a conventional PID controller. In order to obtain the controller parameters on line, many approaches have been developed by several researchers in previous years. We can cite some works such as: PSO-based PID type controller presented by Gaiang [3]; Hybrid genetic algorithm (GA) and bacterial foraging (BF) technique developed by Kim and Cho [4]. Mukherjee and Ghoshal presented a PID Controller for an AVR using Crazyness Based Particle Swarm Optimization (CRPSO) and binary encoded genetic algorithm [5]. Ching-Chang proposed a PID controller for the AVR system based on a real-value genetic algorithm (RGA) and a particle [6] and Dadashpour implemented a PID based on the company's optimization lawless [7], PID for AVR system designed using Taguchi Combined Genetic Algorithm [8], Jingquin Han published several papers on a new unconventional control method such as ADRC [9, 10].

The main contribution of our work consists of two parts: In the first one, the output voltage is regulated by acting on the excitation voltage for a synchronous machine with salient pole rated at power 1.5 kVA using a static excitation. Its control is based on a conventional PI regulator associated with the method PSO to optimize its parameters. The second part deals with a digital ADRC method. The same control methods are applied to a second self-excited synchronous machine with a power of 187 MVA. The obtained results for the ADRC are very satisfactory compared to the PSO heuristic optimization method.

It is useful to organize our work in five sections. After presentation of the state of the art in section one, Some background materials are presented in section two. The second section is devoted to the presentation and modeling of our systems which will be used subsequently in our present study knowing that the first system including a 1.5 KVA power generator with static excitation, it is represented by transfer functions. The second system is a self-excited generator rated at 187MVA, represented in matlab by a simulink model. The parameters of the two machines are given in the appendix.

The third section deals with the application of an AVR controller using the PI and its parameters

optimized by the PSO method. The obtained results for the two generators will be illustrated and analyzed.

The fourth section presents the implementation of the ADRC method in AVR regulator of both studied generators. Some important points and concluding observations of this method are presented. Besides, the two used techniques are analyzed and compared in order to validate our choice.

## II Background Materials

### II.1. Excitation System

The excitation system is developed to supply and regulate the inductive current of the main machine. It consists mainly of an exciter associated with the Automatic Voltage Regulator (AVR) or the power factor regulator. The rectified and filtered terminal voltage of the machine is compared with the reference voltage  $V_{ref}$  to determine the voltage error that is injected to the amplifier of the regulator. This error is introduced to the main damping loop of excitation [13-15].

Another type of excitation system is Static Excitation System that may be used for the high power generator (for our case 187 MVA). It is based on a rectifier using thyristors together with the control system, regulates the excitation voltage  $V_f$ . A schematic diagram of the excitation system is shown in figure 2.

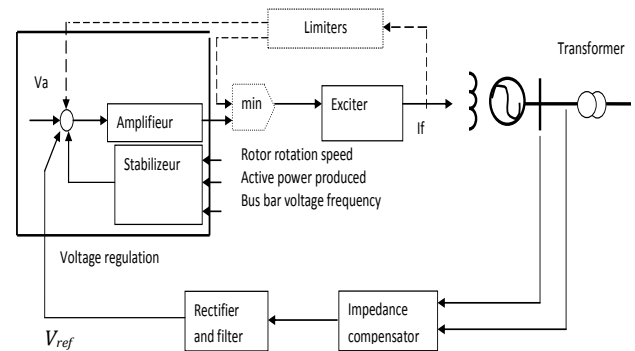


Figure 1. Schematic diagram of the excitation system of low power synchronous machine.

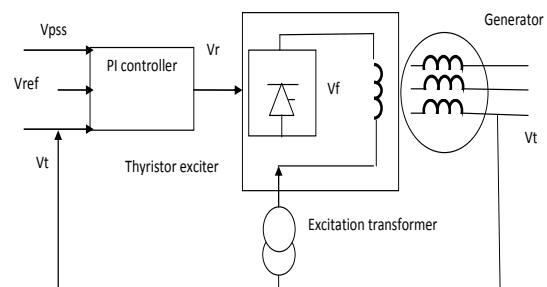


Figure 2. Schematic diagram of the excitation system in power plant

The input voltages to the PI controller such as  $V_t$  and  $V_{pss}$  are compared with the voltage reference  $V_{ref}$ . The output voltage  $V_r$  of the PI controller without internal feedback controls the thyristors of the rectifier using a pulse width modulation (PWM) signal. The regulator is supplied by the generator armature circuit via an excitation step down transformer, adjusted to the parameters of the excitation system. The exciter transformer is used to supply the electrical power to the rectifier as well as a galvanic isolator between high power circuit and the rotor circuit as shown in the schematic diagram of the excitation system of Figure.2 [11, 15, 16].

## II.2. Mathematical Models

For high quality mathematical modeling of a system, all the transfer functions of its main elements should be linearized, by taking into account the major time constants and ignoring the saturation and other non-linearities. The transfer functions of the main elements of the studied system will be represented as follows.

### II.2.1. Excitation System Model

The *excitation system* model is derived from the relationship between the amplification, excitation and compensation functions.

So, the transfer function is:

$$G_E(s) = \frac{K_f}{1+sT_f} \quad (1)$$

### II.2.2. Sensing Circuit Model

The role of the sensing circuit is to rectify, filter and reduce the terminal voltage; its model can be obtained from the first order transfer function:

$$H(s) = \frac{K_r}{1+sT_r} \quad (2)$$

Where,  $T_r$  range is between 0.001 and 0.06 s.

### I.2.3. Generator Model

The simplified transfer function describing the Synchronous Generator is given by:

$$G(s) = \frac{K_G}{1+sT_G} \quad (3)$$

Equation (3) can be derived from Eq. (4) by neglecting  $T_{kd}$  and  $T''_{d0}$ ,

$$G(s) = \frac{K_G(1+sT_{kd})}{(1+sT'_{d0})(1+sT''_{d0})} \quad (4)$$

Where,  $K_G = \frac{x_{md}}{r_f}$ ,  $T'_{d0} = \frac{x_{md}+x_f}{r_f}$ ,  $x_{md} = x_f$  and

$$T_G = T'_{d0} = \frac{x_f}{r_f}.$$

All these parameters can be obtained from experimental tests such as open circuit test, sustained short circuit test, slip test and sudden three phase short circuit test.

### II.2.4. Automatic Voltage Regulator

An automatic voltage regulator (AVR) ensures the internal stability of the closed loop system as well as the attenuation of the influence of disturbances on the output of the controlled system. The PID controller synthesis may be used to improve the dynamic response as well as to reduce or eliminate the steady state error.

The transfer function of a PID-controller is:

$$G_{PID}(s) = K_p(1 + \frac{1}{sT_i} + sT_D) = K_p(\frac{1+sT_i+s^2T_iT_D}{sT_i}) \quad (5)$$

With:  $K_p$  – proportional gain,  $T_i$  – integral constant time,  $T_D$  – derivative constant time.

These parameters can be identified from experimental determined parameters of the laboratory synchronous generator and according to IEEE mathematical relations between leakage inductances.

It can be noted that, even with well-defined systems, tunneling the parameters of the controller is not always easy especially in complex systems.

The model of any system does not always represent the behavior of the system very well during its operation; due to transient phenomena such as non-linearity and / or saturation. Anyway, we will always have a more or less precise idea of the mathematical model that describes the synchronous machine. In order to facilitate the tuning of the controllers, identification methods have been adopted for determining approximately the parameters of the used controller such as Particle Swarm Optimization [17-20].

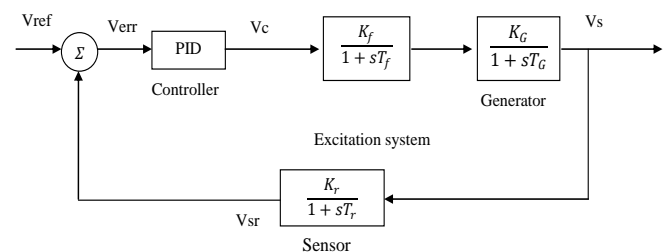


**Figure 3.** Simplified model of the voltage regulator circuit.

## II.3 Particle Swarm Optimization

Particle Swarm Optimization (PSO) is an evolutionary computation algorithm which is founded

upon the principles of biological evolution and is inspired by the study and investigation of swarm patterns occurring in nature [21, 22]. PSO technique was first introduced by Eberhart and Kennedy in 1995 [23, 24]. After that, many researchers have expanded the original idea with alterations ranging from minor parameter adjustments to complete reworking of the algorithm. PSO method is used to explore the search space of a given problem to find the settings or parameters required to maximize or minimize an objective function. It is found to be robust in solving problems featuring nonlinearity and non-differentiability, multiple optima, and large scale system [22].

Particle Swarm Optimization (PSO) is an iterative global search algorithm its goal is to optimize a predefined function called the "fitness" cost criterion or function. It allows an initial set of solutions to evolve towards a final set.

This method is based on the collaboration of individuals with each other. The particles are the individuals and they move in the search hyperspace, while the population is known as (swarm). Each particle moves with each iteration and it closes to the optimum, communicates its position to the others, so that they can modify their trajectories.

This idea is that a group of less intelligent individuals can have a complex global organization. The particle can benefit from the movements of other particles in the same population to adjust its position and speed during the optimization process.

Each individual uses the local information they can access about the whereabouts of their nearest neighbors to decide on their own next move.

To maintain the cohesion of the whole group, very simple rules like "stay close to other particles", "go in the same direction", "go at the same speed" must be respected.

To initiate the algorithm, we use randomness, each particle having a random speed and a position. Then, at each time step:

1. Each particle can assess the quality of its position and it has a memory that allows it to memorize the best point through which it has already passed and it can return back via that point.
2. Each particle is informed of the best point known by its neighborhood.
3. Each particle chooses the best of the best performances of which it knows, modifies its speed according to this information and its own data and moves accordingly. From the disposal information, a particle can decide its next movement as well as its new speed [23].

### II.3.1. Integral Time Multiplied by Square Error (ITSE) Criteria

The objective function is defined from some specifications and desired constraints on the test input signal and some output specifications such as overshoot, rise time, stabilization time and steady state error.

Each performance index has its own advantages and disadvantages and will result in a different system of equation.

The performance criterion used in our research work for the design of the PI controller is the integrated square error of the time weighting (ITSE).

$$ITSE = \int t. e(t)^2 \tag{6}$$

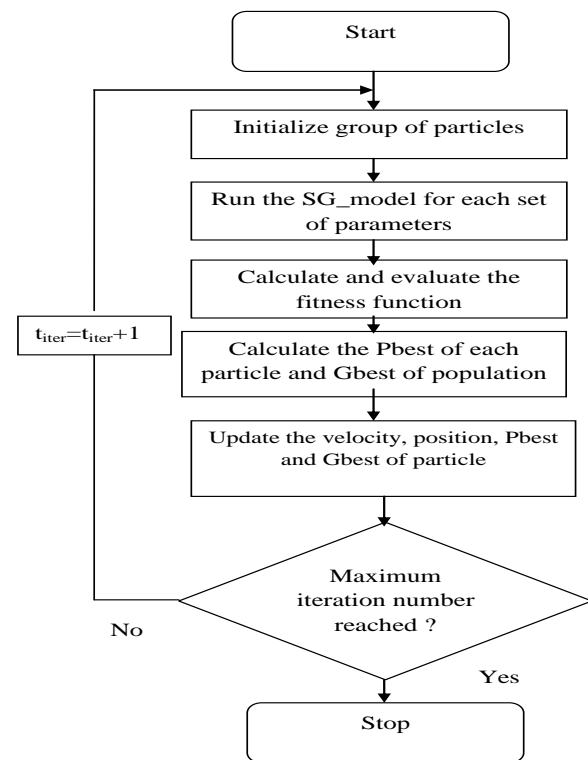


Figure 4. Flowchart for the PSO based PI-controller.

It averages the ISE and ITAE criteria, which amounts, through the action of the time parameter, to a fine analysis of the error at the end of the transient state, while the start is not penalized. It is minimized for a 2nd order of which  $z = 0.58$  [15, 20].

### III AVR Based PI Simulation

The role of AVR is to maintain a constant voltage at the terminals of the synchronous generator (SG) during external disturbances (loads variation, load shedding, and faults....etc.). To test the developed AVR, Simulink model of the complete system has been developed and simulated.

#### III.1. PSO Tuning Results of First Generator

The combination between the SG model and the controller associated with the PSO algorithm allows calculation of the error and the dynamic

characteristics of the system at each position of each particle for each iteration. The PSO parameters are given in table 1.

The idea is to have the best solutions for  $K_p$  and  $K_i$  with graphs of PSO convergence characteristics for different parameters, population size and number of iterations.

The obtained results are shown in figures 5, 6 and 7 [15, 19].

**Table 1.** PSO parameters settings

Number of variables (Dimension of the problem)	2 ( $K_p$ , $K_i$ )
c1	2
c2	2
Velocity updating method	Inertia weight
Wmax	0.9
Wmin	0.4
Correction factor	2.0
Lower bound	[-5.12 -5.12]
Upper bound	[5.12 5.12]
population size	n
number of iterations	t
Fitness function	ITSE

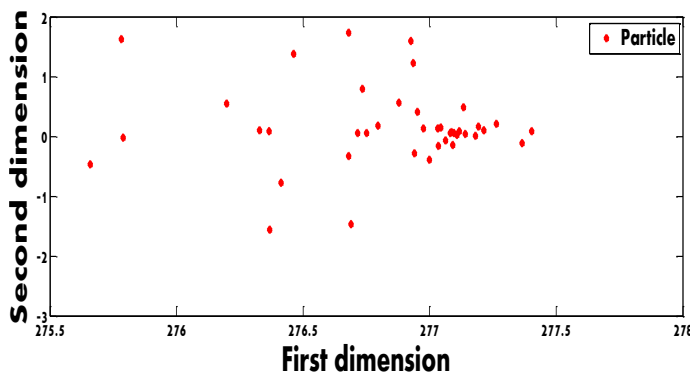
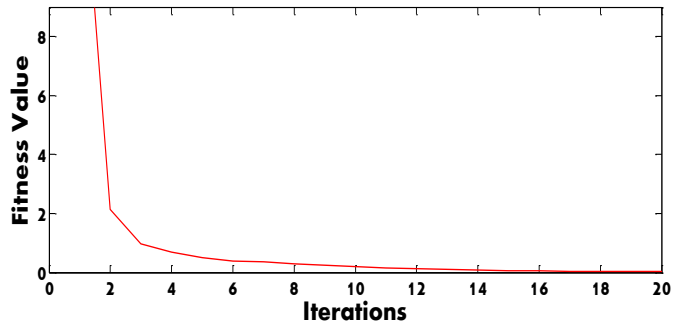
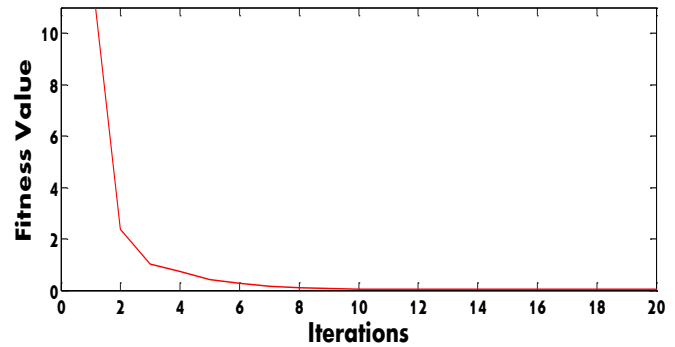


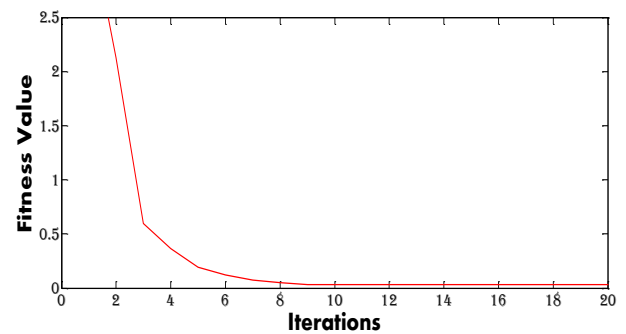
**Figure 5.** Population distribution.



First try:  $K_p=277.1937$ ,  $K_i=0.0149$   
 $n=10$ ,  $t=50$



2<sup>nd</sup> try:  $K_p=277.1963$ ,  $K_i=0.002$   
 $n=20$ ,  $t=100$



3rd try:  $K_p=277.2049$ ,  $K_i=0.0039$   
 $n=50$ ,  $t=100$

**Figure 6.** PSO convergence characteristics and best solutions.

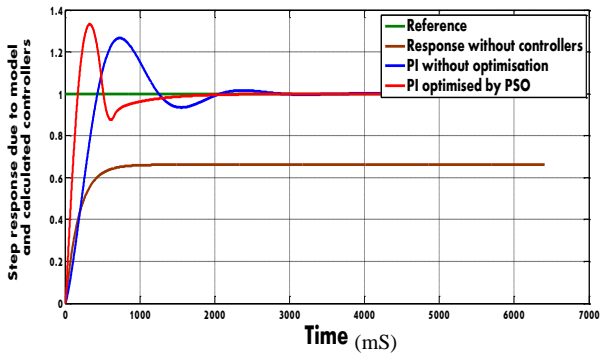


Figure 7. Plot of the step response with and without controller.

Figure 5 presents the population distribution in the space search. The latter is an evolutionary algorithm which uses a population of candidate solutions to obtain optimal solutions of the parameters  $K_p$  and  $K_i$ .

Figure 6 shows the convergence of the fitness function for many population swarms “n” and iterations “t”. It can be noted that the evolution of the objective function towards the global optimum for different populations and iterations can be obtained. The obtained results illustrated in Fig.7 of the first part encouraged us to extend the study for another type of excitation system and another size of synchronous machine, but this time its rated power is in the range of 187 MVA.

**II.2. PSO Tuning Results of the Second Generator**

Figures 8 and 9 represent the application of the full load.

Figures 10 and 11 show the voltage when a ground fault, a short circuit of phase B to the ground, is applied with a ground resistance of  $R = 1 * 10^{-3}$  ohms. It can be noted that the voltage will return rapidly to its initial value after the fault appearance.

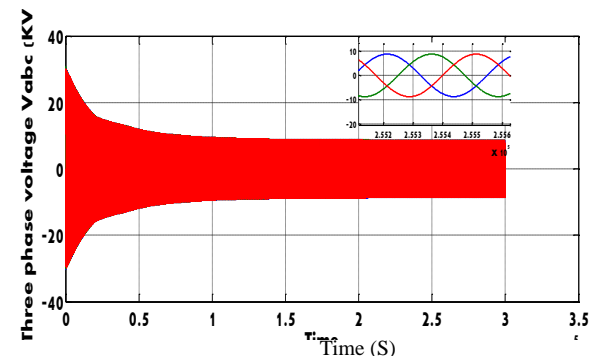


Figure 8. Three phase voltage (KV)

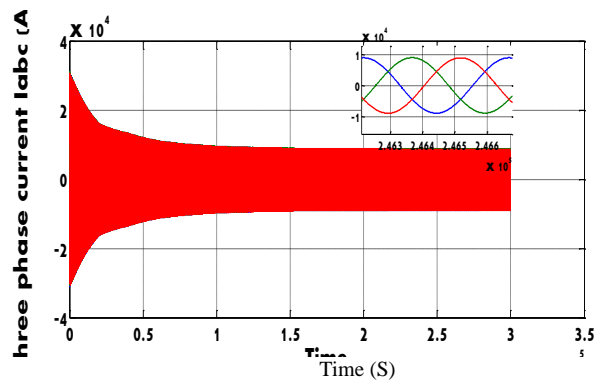


Figure9. Three phase current (A).

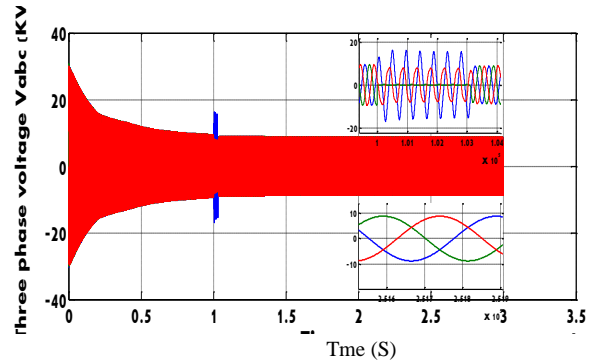


Figure 10. Three phase voltage when a ground fault is applied to phase B at t=1S.

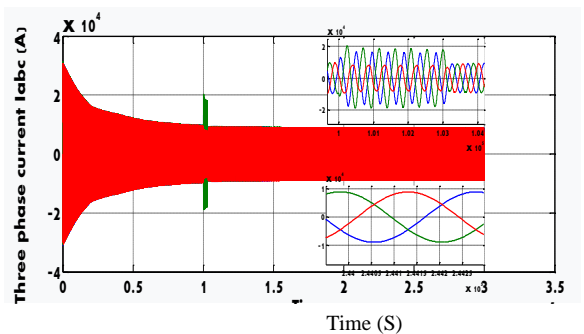


Figure11. Three phase current when a ground fault is applied to phase B at t=1S

**III. Active Disturbance Rejection Control**

Active disturbance rejection control (ADRC) is a new digital control solution, which may replace the widely used conventional controller PID in the 21<sup>st</sup> century, keeping the same advantages of the conventional one, but trying to reduce its disadvantages [10].

ADRC has been proposed by J. Han [9] and simplified by Z. Gao [25, 26]. In order to understand the idea behind this control law, it is necessary to follow the reasoning of J. Han. [10] (Han, 2009) who noticed that the right idea is to understand the two characteristics of PID and its faced challenges. For this reason, all most innovative control methods that have been developed such as adaptive and robust control, aim to have better control performance even

with uncertainties. In this mind, J. Han began the process that ultimately led to the ADRC [27]. Mathematical modeling causes obvious gap which leads to smart implementation and terrible performance. Academic research, so active in automation or modern control for more than fifty years, finds much of its motivation there [28]. Many systems face disturbance phenomena that reduce the precision, the quality of service or even the age of the processes. Control laws that may be developed may take into account the need to improve the performance of new components, machines or complex systems such as energy systems and hence the reduction of the effect on the environment.

This research work aims to improve the precision and robustness of processes in energy production by trying to cancel the influence of disturbances on the behavior of the complete system by designing a controller / observer, using an integrated approach [29].

During the period 1980-1990, Jingquin Han published several papers in a new unconventional control method (Han, 1988, 1995a, b, 2009, 1989). This technique, later called Active Disturbance Rejection Control, which has the advantage of combining the two types of disturbances; the first type of disturbance that is concerning the modeling faults of the system, therefore called internal disturbance, and the second combines those due to noise from the environment, therefore called external disturbance.

The combination of the two types brought J. Han to develop the concept of "total disturbance", which is a fundamental concept of the ADRC. It makes it possible to decouple the control by treating all the unknown coupled dynamics as being a generalized term [27]. The work began with an in-depth state of the art of the operation of the ADRC, which leads to a good complete theoretical understanding of the mathematics governing the controller which is an essential step for synthesizing ADRC controller and hence analyzing the obtained results. Then, the performance can be optimized by setting the appropriate parameters of the controller. First the elements of ADRC will be presented individually and independently.

The ADRC consists of three main elements. The first is a Tracking Differentiator (TD). It is used to extract the derivatives of the reference signal, and then it is used as a reference quantity by the system.

The second component is an Extended State Observer (ESO). This is the heart and keystone of the ADRC, because it estimates the total uncertainty. Finally, the third component is the state error feedback, Linear State Error Feedback (LSEF) or also called Non-Linear State Error Feedback (NLSEF). This part is the same as PID, which has

been modified (in most ADRCs) to take advantage of the power of a nonlinear combination of the output variable, its integral and its derivative.

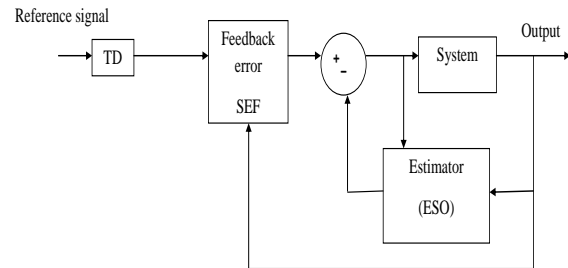


**Figure 12.** ADRC functional block diagram

To review the operation of the ADRC controller, Fig.12 shows the functional block diagram. In the first stage, a reference signal is the input of the block TD and its derivative as an output. In the second stage, thus we will have access not only to the state variables given by the output, but also to their derivatives, which may be essential for the control. The differences between the the state variables and the reference signals will then be injected into the SEF.

The SEF which in turn can get the control as function of these quantities obtained by either linear combination, or non-linear (NLSEF). This control created by the SEF is the desired dynamic of the system. However, external environment disturbances of systems and modeling errors will unfortunately disrupt this dynamic and hence the desired performance can be attained.

ESO estimates in real time the difference between this dynamic and the real dynamic. By correcting the output control of the SEF, therefore, the desired goal is achieved by compensating uncertainties of our system.

In order to design a good ADRC controller that meets the desired performance, whether for its simplicity of implementation and speed, it is therefore necessary to know the specifications of each component (TD, SEF and ESO) [27, 30].

### III.1. State representation of System Model

Consider a system of n order written in the standard form proposed by Han:

$$y^{(n)}(t) = bu(t) + f(t) \quad (7)$$

Whose output quantity is  $y(t)$ , the control quantity  $u(t)$  and  $f(t)$  the quantity defining the total disturbances which will be estimated and rejected after that. The perturbation rejection is completed according to the ADRC as follows:

$$u(t) = \frac{1}{b}(-f_0(t) + u_0(t)) \quad (8)$$

Where,  $f_0(t)$  is estimate of the total disturbance  $f(t)$ , and  $u_0(t)$  is the new control input that will be used to reach the objective.

The substitution of equation (8) in equation (7) gives,

$$y^{(n)}(t) = b \left[ \frac{1}{b} (-f_0(t) + u_0(t)) \right] + f(t) \quad (9)$$

If  $f(t)$  is well estimated by  $f_0(t)$ , and  $f_0(t) = f(t)$ , then, equation (9) can be simplified to:

$$y^{(n)}(t) = u_0(t) \quad (10)$$

From this equation, it can be concluded that if the total disturbance is well estimated, the ADRC control does not require knowledge of any system parameters (without model) to follow the reference value.

This estimation of the total disturbance  $f(t)$  is provided by the extended state observer (ESO).

The equation (11) summarizes the mathematical model of a linear system in state representation,

$$\begin{cases} \dot{x}(t) = Ax(t) + Bu(t) + Eq(t) \\ y(t) = Cx(t) + Du(t) \end{cases} \quad (11)$$

Where:  $x(t)$  is the state vector with the matrix  $A$  which characterizes the internal dynamics of states,  $u(t)$  is the control inputs vector with the matrix  $B$  which characterizes the way in which the control inputs modify the states of the system,  $q(t)$  is the disturbance vector with the matrix  $E$  characterizes the way in which measurable disturbances act on the states of the system, and  $y(t)$  is the output vector. Matrix  $C$  characterizes the evolution of outputs as a function of the states of the system; it is called the output matrix.

The matrix  $D$  characterizes the direct influence of the control quantities on the system outputs; it is a direct connection matrix. When the system is causal the matrix  $D$  is null.

$h(t)$  is set at an unknown function which represents the derivative of the function  $f(t)$ . This function exists because  $f(t)$  depends on the unmodeled dynamics of the system, so it accepts a dynamic that is necessary differentiable. Moreover, the function  $h(t)$  has been introduced just for the needs of state representation; it will not be used in the further development.

The equation (11) becomes:

$$\begin{cases} \dot{x}(t) = Ax(t) + Bu(t) + Eh(t) \\ y(t) = Cx(t) \end{cases} \quad (12)$$

$$\text{Where, } A = \begin{bmatrix} 0 & 1 & 0 & 0 & \dots & 0 \\ 0 & 0 & 1 & 0 & \dots & 0 \\ \vdots & \vdots & \vdots & \ddots & \dots & \vdots \\ 0 & 0 & 0 & 0 & \dots & 1 \\ 0 & 0 & 0 & 0 & \dots & 0 \end{bmatrix},$$

$$B = [0 \ 0 \ \dots \ b \ 0]^T,$$

$$C = [1 \ 0 \ \dots \ 0 \ 0],$$

$$E = [0 \ 0 \ \dots \ 0 \ 1]^T.$$

It can be concluded that only the term  $b$  added by the designer takes place in the control structure [30]. The disturbance rejection control is based on the idea

of formulating a robust control strategy. It aims to compensate for dynamics and disturbances in real time. This approach accurately and quickly estimates disturbances using an extended and compensated non-linear state observer (ESO) during each sampling period to meet the performance requirements of these systems and improve their efficiency [10].

### III.2. Extended State Observer

Knowing that the inputs to ESO are the system output  $y$  and the control signal  $u$ , and the output of ESO provides the important information about  $F$ .

The Luenberger observer that is one of the most famous observers in the state feedback controls has been chosen. It allows reconstructing the state of the system under observation when whole or part of the state vector cannot be measured. It can also estimate the variable or unknown parameters of a system.

A full order Luenberger state-observer can be designed as follows:

$$\begin{cases} \dot{\hat{x}}(t) = A\hat{x}(t) + Bu(t) + L(y(t) - \hat{y}(t)) \\ \hat{y}(t) = C\hat{x}(t) \end{cases} \quad (13)$$

Where  $\hat{x}(t)$  and  $\hat{y}(t)$  represent respectively the dynamics and the output of ESO,  $L$  Correction gain matrix or the observer.

It must emphasize on the term  $L(y(t) - \hat{y}(t))$  which defines the error between the real system and that given by the observer. It can be noted that the good choice of the matrix  $L$  makes it possible to modify the dynamics of the observer which helps us to cancel the error and to converge estimating system to the real one.

### III.3. Sizing of the observer gain L

A well-dimensioned estimator gives a zero error between real system and observable, these results in:

$$(y(t) - \hat{y}(t) = 0 \equiv C(x(t) - \hat{x}(t)) = 0 \quad (14)$$

The error  $\varepsilon(t)$  is the difference between the internal states of the system and those estimated,

$$\varepsilon(t) = x(t) - \hat{x}(t) \quad (15)$$

The derivation of this error gives the difference between the two dynamics describing the two systems:

$$\dot{\varepsilon}(t) = \dot{x}(t) - \dot{\hat{x}}(t) \quad (16)$$

The substitution of equations (12) and (13) in (16), gives:

$$\dot{\varepsilon}(t) = A(x(t) - \hat{x}(t)) - L(y(t) - \hat{y}(t)) \quad (17)$$

(17)

Substituting equations (14) and (15) in (17), we have:

$$\dot{\varepsilon}(t) = (A - LC)\varepsilon(t) \quad (18)$$

Hence, the error is given by the following expression:

$$\varepsilon(t) = e^{(A-LC)t} \quad (19)$$

In order the estimation error tends towards 0 when t increases, it is necessary to choose L, so that the Eigen values of the matrix (A - LC) have strictly negative real parts.

$$VP(A - LC) = (p + \omega_0)^{n+1} \quad (20)$$

Where,  $\omega_0$  is the observer's bandwidth.

Determination of the matrix L helps to find out the observer poles.

All elements of the matrix L depend on a single parameter  $\omega_0$ . Therefore, the adjustment of the observer is conditioned by the choice of its own pulsation  $\omega_0$  with ( $\omega_0 > 0$ ).

The combination of this observer with the control law of equation (2) leads to this final structure of the ADRC control [26] as shown in figure 13.

#### IV. Application of ADRC to our Systems

Based on the previous study, the synthesized ADRC model contains two parts; the first one is a simulink block similar to the one shown in figure 14 and the second is a Matlab program which helps to optimize the performances by adjusting the suitable parameters of the controller (b, w0...) and determine the poles placement of the observer.

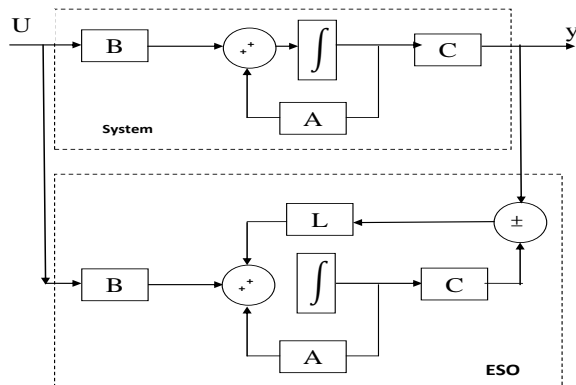


Figure 13. ADRC control structure

First, ADRC controller is associated with the system of figure 3 and using a model of transfer functions. The obtained result is given in figure 15.

In the second part, ADRC controller has been introduced in the system shown in figure 15 using Simulink models as illustrated in figure 14.

Table 2. ADRC parameters settings

	1.5KVA Machine	187MVA Machine
Kp	2.560	0.0025
Kd	2.336	10 <sup>-3</sup>
b	3	15
$\omega_0$	50	1.8
$\omega_c$	1.5	0.05

With  $\omega_c$  : the controller bandwidth

#### IV.1 Simulation Results and Discussion

##### IV.1.1 1.5 KVA synchronous machine case

The responses of the system with PID optimized by PSO (PID-PSO) and ADRC control are illustrated in figure 17.

From table 3, the settling time for PID-PSO and ADRC are 1.887 sec and 0.77 sec respectively. PID-PSO of 33% overshoot, but ADRC has 11% of overshoot. The both methods produce a zero error in steady-state.

The comparison is made between the results of PID-PSO and ADRC for same conditions.

Our objective is to control and maintain the steady state voltage equal to the reference one with a tolerance of  $\pm 2\%$ .

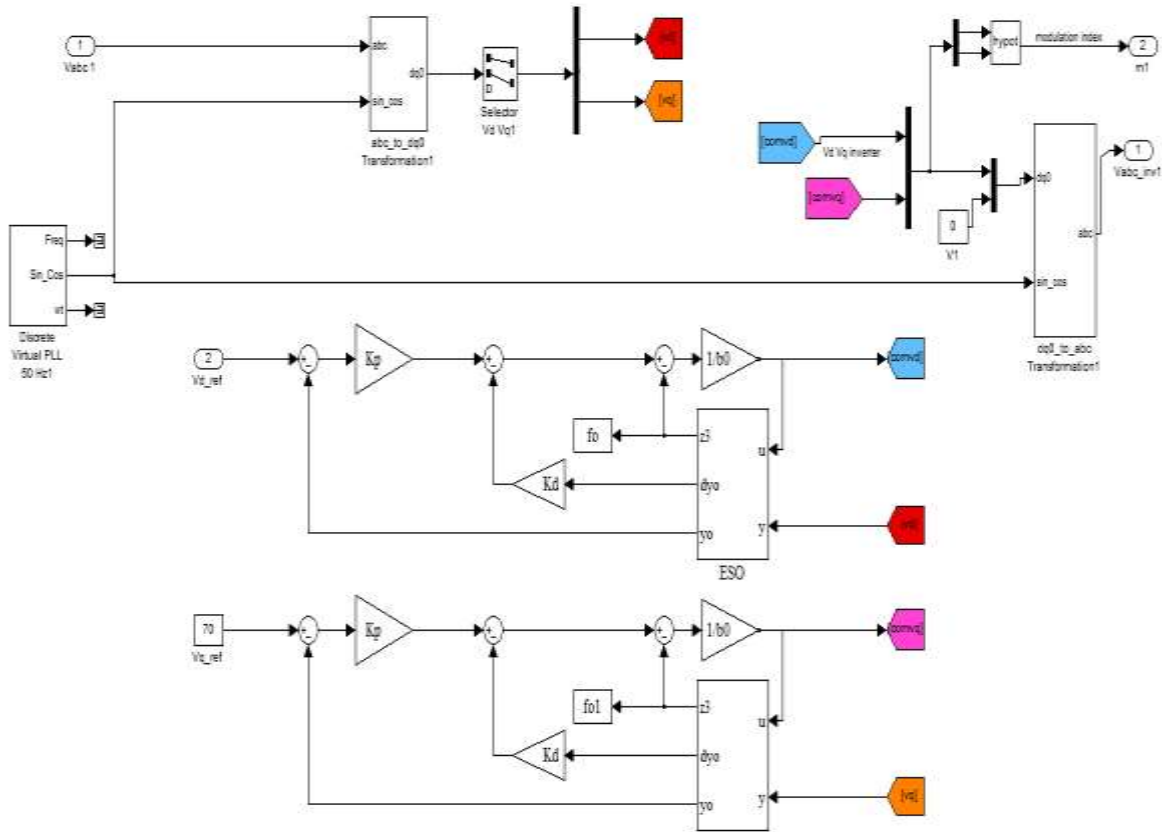


Figure14. ADRC Simulink model

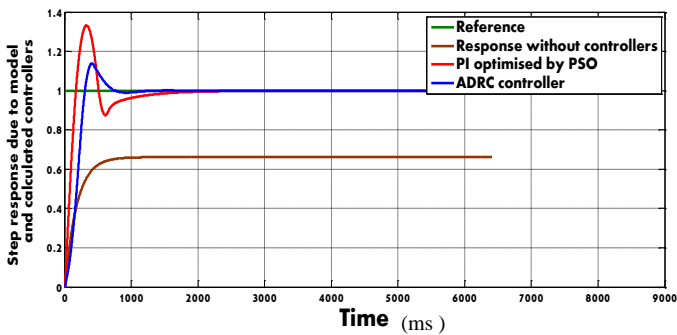


Figure15. Plot of the step response due to the model and calculated regulators for the first system

Table 3. Comparison of the control performance of the AVR system controlled by different controllers

Performance	overshoot	Settling time	Steady state error
Type			
PI optimized by PSO	33%	1.887	0
ADRC control	11%	0.77	0

#### IV.1.2 187MVA synchronous machine case

A ground fault (short circuit) with a grounding resistance of  $R = 1 \cdot 10^{-3}$  ohms is applied at  $t=1.8$ . Figures 16 and 17 show the voltage when a ground fault, a short circuit of phase B to the ground, is applied with a ground resistance of  $R = 1 \cdot 10^{-3}$  ohms. It can be noted that the voltage will return rapidly to its initial value after the fault appearance.

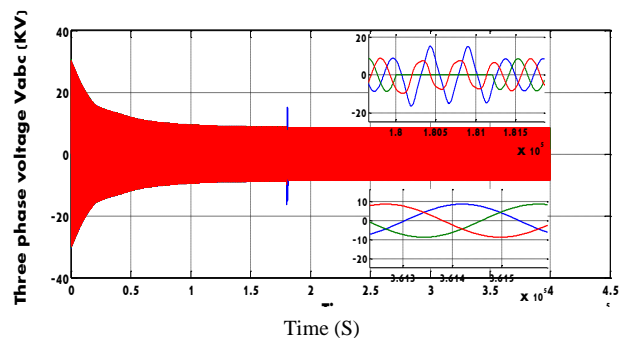


Figure 16. Three phase voltage when a ground fault is applied to phase B at  $t=1.8$  S for the second generator.

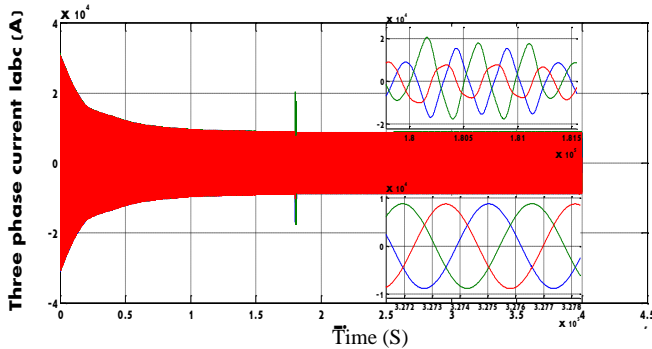


Figure 17. Three phase current when a transient ground fault is applied to phase B at  $t=1.8$  S.

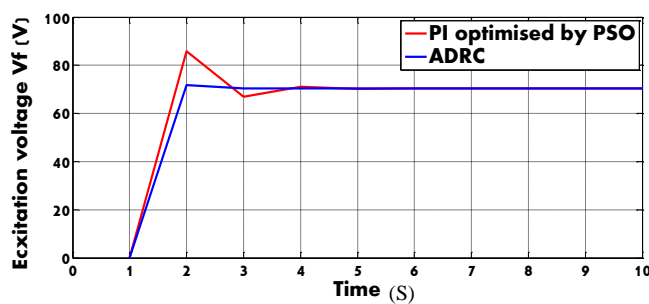


Figure 18. Excitation voltage  $V_f$  (V) with PSO and ADRC for the second generator.

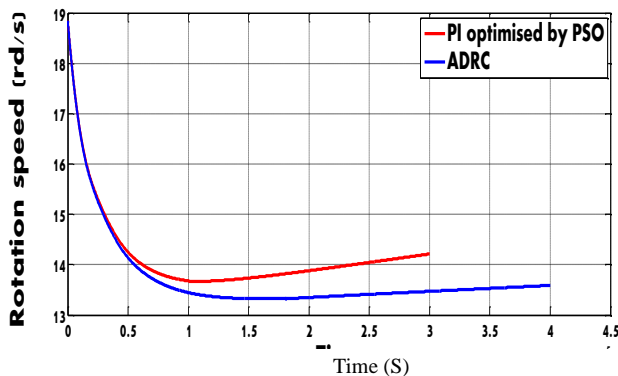


Figure 19. Speed  $w$ (rd/s) with ADRC and PID-PSO for the second system

The Simulation results verify the efficiency of the ADRC which maintains the voltage at nominal value despite the presence of various disturbances. They also demonstrate that ADRC has better setpoint tracking and robust performance than PID-PSO. The good tracking of the voltage reference and the response speed of the dynamics are ensured by the ADRC controller, compared to the PI regulator, which can be shown in Figures 18 and 19.

## V. Conclusion

Most of the existing control design methods are based on mathematical modelling of the system. However, many real systems are highly uncertain, their accurate models have not yet been developed, and disturbances are unknown.

In first step, the PI gains have been defined based on PSO heuristic algorithm. The connection between the control unit and the power circuit for the first machine is made by a triggering circuit which is designed and implemented on the basis of a ramp comparator strategy during the implementation [16]. For the second self-exciting machine, the simulation is done with the PI characteristics based on the AVR using Matlab software.

After adopting another type of controller relatively recent and still little used to date ADRC. This type of controller estimates and cancels or compensates global disturbances directly. It requires very little information about the plant. Then, the controller uses the needed information provided by the estimator to control the system independent on the mathematical model.

The ADRC controller is classified among the controllers which don't require the system model. In our case, we have worked on so-called gray box systems where the majority of these parameters are known. This controller type effectively corrects the voltage level and compensates for disturbances of the complex and nonlinear system [31].

It can be noted that the optimization of PI controller by the PSO method has lead to the best performance of PI, which has been proven. But the PI has limits such as in the case of non-linear, noisy and / or uncertain systems. Such complications can be brought by the integral term and the loss of performance in the combination of the proportional and integral terms.

It can also be noted that ADRC gives better results without time-consuming adjustment step, knowing that the setpoint tracking is faster and more accurate. Therefore, the simulation results show that the ADRC control is more efficient than the PI-PSO control.

## Acknowledgements

I would like to thank Professor R. MANSOURI from Mouloud Mammeri University for his help and these guidelines during my preparation of this article.

VI. References

1. Bendjeh, O.; Ishak Boushaki, S. Bat algorithm for optimal tuning of PID controller in AVR system. International conference on control, Engineering and information technology (2014) 158:170.
2. Ahcene, F.; Bentarzi, H. Automatic voltage regulator design using particle swarm optimization. International conference on electrical engineering (2020).
3. Gaiang, Z.L. A particle swarm optimization approach for optimum design of PID controller in AVR system, IEEE Transactions on Energy Conversion 19 (2004) 348:391.
4. Kim, D.H.; Cho J.H. A biologically inspired intelligent PID controller tuning for AVR systems. International Journal of Control Automatic and Systems 4 (2006) 624:636
5. Mukherjee V Ghoshal, S.P. Intelligent particle swarm optimized fuzzy PID controller for AVR system. Electric Power System Research 77 (2007) 1689:1698.
6. Wong, C.C.; Li, S.A Y.; Wang H. Optimal PID controller design for AVR system. Tamkang Journal of Science and Engineering; 12 (2009) 259:270.
7. Shayeghi, H.; Dadashpour, J. Anarchic Society Optimization Based PID Control of an Automatic Voltage Regulator (AVR) System. Electrical and Electronic Engineering 2 (2012) 199:207.
8. Hasanien, H. M. Design optimization of PID controller in automatic voltage regulator system using taguchi combined genetic algorithm method. IEEE Systems Journal 7 (2013) 825:831.
9. Han, J. A class of extended state observers for uncertain systems. control and decision 10 (1995) 85:88.
10. Han, J. From PID to active disturbance rejection control. IEEE Transactions on industrial electronics 56(2009) 900:906.
11. Ygzaw, A.; Banteyirga. B.; Darsema, M. Generator excitation loss detection on various excitation systems and excitation system failure, ICST 2020 Springer nature switzerland AG. LNICST308(2020) 382 :394.
12. Wei, Y.; Zheng, Xu. Excitation System Parameters Setting for Power System Planning. Power Engineering Society Summer Meeting, IEEE (2002).
13. Paszek, S.; Bobon, A.; Berkansen, S.; Majka, L.; Nocon, A.; Pruski, P. Synchronous generator and excitation systems operating in power system», Springer 631(2020) 49:149.
14. Barakat, A.M. Contribution à l'amélioration de la régulation de tension des générateurs synchrones: nouvelles structures d'excitation associées à des lois de commandes  $H_{\infty}$ . Poitiers university (2011).
15. Van Custem, T. Introduction to electric power and energy systems. Montefiore Liège université science appliqués (2019).
16. Shi, Y.; Eberhart, R. A modified particle swarm optimizer. Proceedings of IEEE World Congress on computational intelligence international conference on evolutionary computation (1998) 69:73.
17. Ramirez, JM.; Montalvo.; Nuno, CI. Modelling synchronization and implementation of the virtual synchronous generator: a study of its reactive power handling, Springer verlag GmbH germany part of springer nature (2020).
18. Derrar, A. Résolution du problème d'optimisation  $H_{\infty}$  des stabilisateurs PSS robustes par les approches métaheuristiques. Sidi bel abbes university (2016).
19. Teodor Wisniewski, M. Modélisation non-linéaire des machines synchrones pour l'analyse en régime transitoires et les études de stabilité. Université Paris-Saclay (2018).
20. Hashemi, F.; Mohammadi, M. Combination of continuous action reinforcement learning automata on PSO to design PID controller for AVR system. IEE TRANSACTIONS 28 (2015) 52:59.
21. Clerc, M.; Kennedy, J. The particle swarm explosion stability and convergence in a multidimensional complex space. IEEE Transactions on Evolutionary Computation 6 (2002) 58:73.
22. Cristian, B.; Merkle, D. Swarm Intelligence: Introduction and Applications Natural Computing Series, Springer-Verlag Berlin Heidelberg (2008).
23. Kennedy, J.; Eberhart, R. Particle swarm optimization. Proc IEEE IntConf Neural Netw 4(1995) 1942:1948.
24. Carlisle, A.; Dozier, G. An off-The-Shelf PSO. Workshop particle swarm optimization Indianapolis (2001).
25. Gao, Z.; Huang, Y.; Han, J. An alternative paradigm for control system design. In proceeding of the 40th IEEE conference on decision and control 5(2001) 4578:4585.
26. Martini, A.; Leonard, F.; ABBA, G. Modélisation et commande d'un hélicoptère drone soumis à des rafales de vent. 18<sup>ème</sup> congrès français de mécanique (2007).
27. Vincent, D. Commande d'un quadrioptère par rejet de perturbations. Ecole polytechnique de Montréal (2008)
28. Fliess, M.; Join, C. Two competing improvement of PID controllers. IST Open science London UK (2017).
29. Gonzalez, J. Estimation et controle des systems dynamiques à entrée inconnues et energies renouvelables. Centrale Lille (2019).
30. Wen, T.; Caifen, F. Linear active disturbance rejection control : analyse and tuning via IMC. IEE Transactions on industrial electronics 63 (2016) 2350 :2359.
31. Mandali, A.; Dong, L.; Morinec, A. Robust controller design for automatic voltage regulation. American control conference Denver 1-3 (2020) 2617:2622.

VII. Appendix

Table 4. 1.5kVA salient-pole Lab-Volt SG parameters [2].

Nominal rms line-to-neutral voltage	$U_n$	220 v
Frequency	$f_n$	50 Hz
Stator resistance	$R_s$	2.2 $\Omega$
Rotor resistance	$R_f$	127 $\Omega$
Direct-axis synchronous reactance (unsaturated)	$X_d$	75.443 $\Omega$
Quadrature-axis synchronous reactance (unsaturated)	$X_q$	46.556 $\Omega$
Direct-axis open-circuit time constant	$T_{do}'$	0.235 s
Direct-axis transient reactance	$X_d'$	10.309 $\Omega$
Direct-axis transient time constant	$T_d'$	0.0776 s
Direct-axis sub-transient reactance	$X_d''$	8.5298 $\Omega$
Quadrature-axis sub-transient reactance	$X_q''$	5.2637 $\Omega$
Direct-axis sub-transient time constant	$T_d''$	0.0147 s

*Table 5. 187M VA SG parameters*

Nominal power	$P_n$	$187*10^6VA$
Nominal rms line-to-neutral voltage	$U_n$	$13800 v$
Frequency	$f$	$60 Hz$
Stator resistance	$R_s$	$2.9*10^{-3} \Omega$
Rotor resistance	$R_f$	$5.9*10^{-4} \Omega$
Stator leakage inductance	$L_l$	$3.089*10^{-4} H$
Direct-axis synchronous magnetizing inductance	$L_{md}$	$3.21*10^{-3} H$
Quadrature-axis synchronous magnetizing inductance	$L_{mq}$	$9.71*10^{-4} H$
Field leakage inductance referred to the stator	$L_{fd}'$	$3.0712*10^{-4} H$
Direct-axis damper resistance	$R_{Kd}'$	$1.019 10^{-2} \Omega$
Direct-axis damper leakage inductance	$L_{LKd}'$	$4.91*10^{-4} H$
Quadrature-axis damper resistance	$R_{Kq1}'$	$2.008 10^{-2} \Omega$
Quadrature-axis damper leakage inductance	$L_{LKq1}'$	$1.03*10^{-3} H$
inertia	$J$	$3.89*10^6 Kg.m^2$
Pole pair	$p$	$20$

**Please cite this Article as:**

Ahcene F., Bentarzi H., Ouadi A., Automatic Voltage Regulator Design Enhancement Taking Into Account Different Operating Conditions And Environment Disturbances, *Algerian J. Env. Sc. Technology*, 9:2 (2023) 3048-3060